Large-amplitude motion of a compressible fluid in the atmosphere

By ALFONS J. CLAUS
Bell Telephone Laboratories, Whippany, New Jersey

(Received 20 June 1962 and in revised form 6 June 1963)

Large-amplitude atmospheric flows past mountain ridges are investigated. The flows are assumed to be steady and two-dimensional. Diffusive and viscous effects are neglected but static compressibility is taken into account.

The larger part of the investigation is devoted to the study of waves in the lee of mountain ridges. The major contribution consists in the treatment of the large-amplitude motion. The flows are governed by an equation which turns out to be linear for certain upstream conditions. These conditions impose some restrictions on the wind profile and stratification of the entropy and specific energy far upstream. However, flow patterns representing realistic upstream conditions have been obtained.

A comparison between a compressible flow and an incompressible flow with equivalent upstream conditions is included.

1. Introduction

This is an investigation of large-amplitude atmospheric flows past mountain ridges. The flows are assumed to be steady and two-dimensional. Since diffusive and viscous effects are of minor importance in large-scale atmospheric phenomena, they are neglected. The compressibility of the air is taken into account. However, effects of dynamic compressibility will be ignored because the Mach number can be assumed everywhere small. This is equivalent to assuming that any change in density of a fluid element is entirely due to a change in its elevation.

The larger part of this investigation is devoted to the study of waves in the lee of mountain ridges. The presence of these waves is in essence a result of the non-homentropy and non-homenergy of the atmosphere. However, the analysis of non-homentropic flows is greatly complicated by the lack of a unique relationship between pressure and density, valid throughout the whole field of flow. Several authors (Lyra, Queney, Scorer, Crapper) have studied the subject by perturbation methods, and their results are valid only when the disturbances are small compared with the corresponding quantities in the undisturbed flow. The major contribution of the present investigation consists in the treatment of the large amplitude motion. In the study to be presented here, the flows are governed by an equation whose form depends on the conditions far upstream of the mountain ridge. Some of these conditions make the latter equation linear provided stratifications of entropy and specific energy are slight, and the Mach number is indeed everywhere small as assumed. These particular upstream conditions thus give rise to large-amplitude flows which are still governed by a linear equation.

The linearity of the equation imposes some restrictions on wind profile and stratification of the relevant physical quantities far upstream of the ridge. However, the method has proved to be quite flexible and several flow patterns have been obtained corresponding to various upstream conditions which are realistic.

In order to investigate the effect of compressibility, two flow patterns with equivalent upstream conditions, one for a compressible fluid and the other for an incompressible fluid, were obtained and compared with each other. A discussion of equivalent upstream conditions is included.

2. The governing differential system

The equations of motion for steady two-dimensional flows of an inviscid fluid are

$$u_1\frac{\partial u_1}{\partial x_1}+u_3\frac{\partial u_1}{\partial x_3} = -\frac{1}{\rho_*}\frac{\partial p_*}{\partial x_1}, \tag{1a}$$

and

$$u_1\frac{\partial u_3}{\partial x_1}+u_3\frac{\partial u_3}{\partial x_3} = -\frac{1}{\rho_*}\frac{\partial p_*}{\partial x_3}-g, \tag{1b}$$

where (u_1, u_3), are the velocity components in the (x_1, x_3) directions, ρ_* the density and p_* the pressure. The equation of continuity is

$$\frac{\partial(\rho_* u_1)}{\partial x_1}+\frac{\partial(\rho_* u_3)}{\partial x_3} = 0. \tag{2}$$

If diffusive effects are neglected the quantity p_*/ρ_*^γ is constant along a pathline and so, for steady flows, constant along a streamline. However, for the flow of a non-homentropic fluid considered here, the value of p_*/ρ_*^γ changes from streamline to streamline. Therefore ρ_* is not a function of p_* alone throughout the whole field of flow, and the expression dp_*/ρ_* is not a total differential. This major difficulty can be avoided by introducing an associated flowfield which is related to the old one by means of a transformation due to Yih (1960*a*)

$$u_1' = u_1\sqrt{\lambda}, \quad u_3' = u_3\sqrt{\lambda}, \quad \rho_*' = \rho^*/\lambda, \quad p_*' = p_*,$$

with

$$\lambda = \frac{\rho_*}{\rho_0}\left(\frac{p_0}{p_*}\right)^{1/\gamma}.$$

When these changes of dependent variables are used, equations (1*a*) and (1*b*) become

$$u_1'\frac{\partial u_1'}{\partial x_1}+u_3'\frac{\partial u_1'}{\partial x_3} = -\frac{1}{\rho_*'}\frac{\partial p_*'}{\partial x_1} \tag{3a}$$

and

$$u_1'\frac{\partial u_3'}{\partial x_1}+u_3'\frac{\partial u_3'}{\partial x_3} = -\frac{1}{\rho_*'}\frac{\partial p_*'}{\partial x_3}-g\lambda, \tag{3b}$$

in which ρ_*' now depends solely on p_*'. Indeed

$$\rho_*' = \frac{\rho_*}{\lambda} = \rho_0(p_*'/p_0)^{1/\gamma}. \tag{4}$$

The equation of continuity becomes

$$\frac{\partial(\rho'_* u'_1)}{\partial x_1}+\frac{\partial(\rho'_* u'_3)}{\partial x_3}=0. \tag{5}$$

Equation (5) guarantees the existence of a stream function $\psi'_*(x_1, x_3)$ in terms of which the velocity components can be expressed as

$$u'_1=\frac{\rho_0}{\rho'_*}\frac{\partial\psi'_*}{\partial x_3},\quad u'_3=-\frac{\rho_0}{\rho'_*}\frac{\partial\psi'_*}{\partial x_1}. \tag{6}$$

This stream function can be shown to satisfy the equation

$$\nabla^2_*\psi'_*-\frac{1}{\rho'_*}\left(\frac{\partial\rho'_*}{\partial x_1}\frac{\partial\psi'_*}{\partial x_1}+\frac{\partial\rho'_*}{\partial x_3}\frac{\partial\psi'_*}{\partial x_3}\right)+gx_3\frac{\rho'^2_*}{\rho_0^2}\frac{d\lambda}{d\psi'_*}=\frac{\rho'^2_*}{\rho_0^2}\frac{dH'_*}{\partial\psi'_*}, \tag{7}$$

where
$$H'_*=\frac{\gamma p_0}{(\gamma-1)\rho_0}\left(\frac{p'_*}{p_0}\right)^{(\gamma-1)/\gamma}+\frac{q'^2_*}{2}+g\lambda x_3. \tag{8}$$

With the neglect of dynamic compressibility and the assumption of small variations of H'_* and λ, equation (7) can be written as†

$$\nabla^2_*\psi'_*+\frac{1}{\gamma-1}\frac{g}{H'_*-gx_3}\frac{\partial\psi'_*}{\partial x_3}+gx_3\left(\frac{H'_*-gx_3}{K}\right)^{2/(\gamma-1)}\frac{d\lambda}{d\psi'_*}=\left(\frac{H'_*-gx_3}{K}\right)^{2/(\gamma-1)}\frac{dH'_*}{d\psi'_*}, \tag{9}$$

in which
$$K=\frac{\gamma p_0}{(\gamma-1)\rho_0}.$$

The functions $\lambda(\psi'_*)$ and $H'_*(\psi'_*)$ are to be considered as known and are conveniently determined far upstream.

Equation (9) will be used for the study of two-dimensional, atmospheric flows past mountain ridges. Except for the obstacle (mountain profile), the ground will be considered perfectly level which implies that the stream function $\psi'_*(x_1, x_3)$ on the level portion of the ground is equal to a constant and can be taken equal to zero.

The fact that there is no rigid upper boundary for the atmosphere causes some difficulty. However, because of the very stable stratification in the constant temperature stratosphere, vertical motion in that layer is somewhat inhibited. If we assume no vertical displacement in the stratosphere, the interface between the troposphere and stratosphere may be considered to be a rigid plane. The flows studied under this assumption are therefore restricted to the troposphere. If d is the height of this interface (the tropopause), this assumption is mathematically equivalent to $\psi'_*(x_1, d)=$ const., which is a second boundary condition for $\psi'_*(x_1, x_3)$. With the dimensionless variables

$$x=x_1/d,\quad z=x_3/d,\quad \psi'=\psi'_*/d(gd)^{\frac{1}{2}},\quad H'=1/\alpha=H'_*/gd,$$
$$\beta=\left(\frac{\gamma-1}{\gamma}\right)^{2/(\gamma-1)}\left(\frac{\rho_0 H'_*}{p_0}\right)^{2/(\gamma-1)},\quad (u,w)=\frac{(u_1,u_3)}{(gd)^{\frac{1}{2}}},$$

† For the derivation of equations (7) and (9) and a discussion of the underlying assumptions we refer to Yih (1960*a*). A vorticity equation equivalent to (7) was given by Long (1953*c*), who also considered the flow of two superposed homentropic layers over a barrier.

equation (9) can be put in the form

$$\nabla^2\psi' + \frac{1}{\gamma-1}\frac{\alpha}{1-\alpha z}\frac{\partial\psi'}{\partial z} + \beta z(1-\alpha z)^{2/(\gamma-1)}\frac{d\lambda}{d\psi'} = \beta(1-\alpha z)^{2/(\gamma-1)}\frac{dH'}{d\psi'}. \tag{10}$$

The boundary conditions become

$$\psi'(x,0) = 0 \tag{11a}$$

for values of x corresponding to the level portion of the ground, and

$$\psi'(x,1) = \text{const.} \tag{11b}$$

The atmosphere has thus been replaced by a mathematical model (figure 1) in which the essential physical features have been retained and should be quite adequate for the study of atmospheric flows over mountain ridges. This mathematical model consists of a channel bounded by two rigid horizontal planes

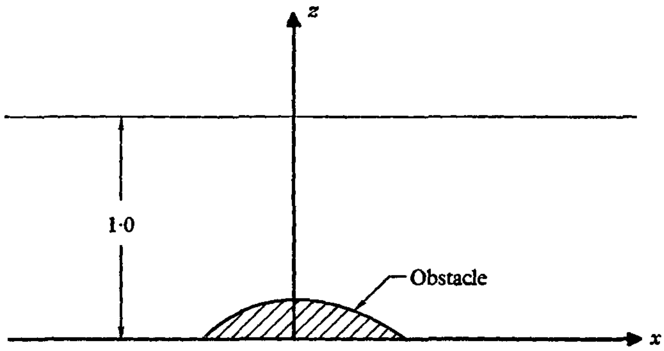

FIGURE 1. Mathematical model for the study of two-dimensional flows in the troposphere.

located at $z = 0$ and $z = 1$ in a rectangular Cartesian co-ordinate system. An obstacle is present on the lower boundary. The flow is governed by the system consisting of equations (10) and (11). The form of equation (10) depends on the upstream conditions since they determine the functions $d\lambda/d\psi'$ and $dH'/d\psi'$. These conditions will be discussed in some detail in the next section.

3. Upstream conditions leading to a linear differential equation

In order to have a clear physical picture of what is meant by conditions upstream, a uniform flow between the two rigid planes ($z = 0$ and $z = 1$) with no obstacle present can be considered. It is obvious that the pressure, density, temperature and velocity profiles do not depend on the section at which they are taken. Suppose that, at a certain time, an obstacle is introduced. If the resulting unsteady flow tends to a steady state, and furthermore if the introduction of the obstacle does not alter the distributions of p, ρ, T and U sufficiently far upstream, the conditions far upstream can be considered as pre-assigned.

First of all let it be observed that, of the four functions, $p(z)$, $\rho(z)$, $T(z)$, $U(z)$, only two can be chosen arbitrarily, namely, the velocity $U(z)$ and any one of $p(z)$, $\rho(z)$ and $T(z)$, say $\rho(z)$. Indeed, since far upstream the flow is uniform, the pressure p can be obtained from ρ by means of the equation $dp/dz = -(g\rho_0 d/p_0)\rho$. The temperature T follows then from the gas law.

If the velocity and density are given (as functions of z) far upstream, all the four quantities p, ρ, T and U are known and λ can be determined from $\lambda = \rho p^{-1/\gamma}$. The specific energy H' can then be evaluated using the relation

$$H' = Ep^{(\gamma-1)/\gamma} + \tfrac{1}{2}\lambda U^2 + \lambda z, \tag{12}$$

in which

$$E = \frac{\gamma p_0}{(\gamma-1)\rho_0 g d}.$$

Furthermore, far upstream, $U' = U\sqrt{\lambda}$ and ψ' are related by

$$U' = \frac{1}{\rho'}\frac{d\psi'}{dz} = \frac{\lambda}{\rho}\frac{d\psi'}{dz} \quad \text{or} \quad U = \frac{\sqrt{\lambda}}{\rho}\frac{d\psi'}{dz},$$

or

$$\psi' = \int_0^z \frac{\rho U}{\sqrt{\lambda}}\,dz.$$

We have thus H', λ and ψ' as functions of z far upstream and H' and λ can be determined as functions of ψ'. The latter functional relationships are valid throughout the whole field of flow, and, as pointed out earlier, they determine the form of the governing differential equation.

In the search for a solvable system we will try to obtain linear functions of ψ' for $d\lambda/d\psi'$ and $dH'/d\psi'$. Clearly, a random choice of the upstream density ρ and velocity U would, in general, not lead to a linear dependence of $dH'/d\psi'$ and $d\lambda/d\psi'$ on ψ'. The adopted scheme will therefore be an inverse one. Since we have the choice of two arbitrary functions (for instance, U and ρ) of z, we shall so choose them as to insure the linear dependence of $dH'/d\psi'$ and $d\lambda/d\psi'$ on ψ'. Thus, we put (Yih 1960*a*).

$$\frac{d\lambda}{d\psi'} = A\psi' + B \tag{13a}$$

and

$$\frac{dH'}{d\psi'} = C\psi' + D. \tag{13b}$$

Once the constants A, B, C, D are chosen, it is possible to determine the upstream situation. That this is indeed so can best be shown by determining the upstream conditions corresponding to a certain choice of A, B, C, D which will now be done.

Inserting the expressions (13) for $d\lambda/d\psi'$ and $dH'/d\psi'$ into equation (10), we obtain

$$\nabla^2\psi' + \frac{1}{(\gamma-1)}\frac{\alpha}{(1-\alpha z)}\frac{\partial\psi'}{\partial z} + \beta(1-\alpha z)^{2/(\gamma-1)}(Az-C)\,\psi' = \beta(1-\alpha z)^{2/(\gamma-1)}(D-Bz). \tag{14}$$

Since the flow far upstream is essentially uniform, the stream function becomes a function of z alone, say $\psi_1'(z)$, and is governed by

$$\frac{d^2\psi_1'}{dz^2} + \frac{1}{(\gamma-1)}\frac{\alpha}{(1-\alpha z)}\frac{d\psi_1'}{dz} + \beta(1-\alpha z)^{2/(\gamma-1)}(Az-C)\,\psi_1' = \beta(1-\alpha z)^{2/(\gamma-1)}(D-Bz), \tag{15}$$

which is an ordinary differential equation for $\psi_1'(z)$. Any function $\psi_1'(z)$ satisfying (15) guarantees the linearity of (10). Once $\psi_1'(z)$ is known, λ and H' as functions of z (far upstream) are easily determined. Indeed it follows from (13*a*) and (13*b*) that

$$\lambda = \tfrac{1}{2}A\psi_1'^2 + B\psi_1' + \lambda_0, \tag{16a}$$

and

$$H' = \tfrac{1}{2}C\psi_1'^2 + D\psi_1' + H_0'. \tag{16b}$$

The constant λ_0 can be chosen to make $\lambda = 1$ at the reference point, i.e. the point where the pressure and density are p_0 and ρ_0, respectively. This point has been taken at $z = 0{\cdot}5$ in our calculations. The constant H_0' has to be taken in such a way as to make $\alpha \approx 1/H'$. Since one of the earlier assumptions was that the variation in H' is small, $\alpha = 1/H'$ was treated as a constant in equation (15). By selecting H_0' as indicated, H' (slightly varying with height) will be consistent with the value of α appearing in (15).

It follows from (12) that

$$p = \left[\frac{H' - \lambda z - \frac{1}{2}U'^2}{E}\right]^{\gamma/(\gamma-1)}. \tag{17}$$

Furthermore

$$U' = p^{-1/\gamma}\frac{d\psi_1'}{dz}. \tag{18}$$

The only unknowns appearing in equations (17) and (18) are p and U'. Since U'^2 is usually very small with respect to the other terms in (17), the system can best be solved using an iterative scheme. Once U' and p are known, the velocity U and density ρ follow then from $U = U'/\sqrt{\lambda}$ and $\rho = \lambda p^{1/\gamma}$.

The previously obtained pressure $p(z)$ and density $\rho(z)$ satisfy the equation of static equilibrium $dp/dz = -(g\rho_0 d/p_0)\rho$. This is indeed guaranteed by the fact that equation (15) is the equation of static equilibrium in terms of the stream function $\psi_1'(z)$.

Since equation (15) does not uniquely determine $\psi_1'(z)$, the same set of values of A, B, C and D corresponds to different upstream conditions and therefore leaves this inverse procedure quite flexible. It may thus be hoped that a realistic upstream situation can be found, first by selecting proper values for A, B, C and D and further, once a definite choice has been made, by taking the most suitable solution of (15).

Equation (15) has been solved by a series method. Various realistic upstream conditions have been obtained. Some of them are shown in figure 2. In all cases the density stratification fits meteorological data very closely. This density stratification is quite independent of the values of A, B, C and D as long as the velocity is kept within reasonable limits. Furthermore, these coefficients by no means determine the stratification in entropy and specific energy, but merely establish some relationship between this stratification and the velocity. Roughly an increase in the velocity leads, for constant A, B, C and D, to a greater stratification. Entropy-stratification and wind profiles actually occurring in the atmosphere can be approximated quite closely as can be seen from figure 2. The present analysis is therefore not without practical value.

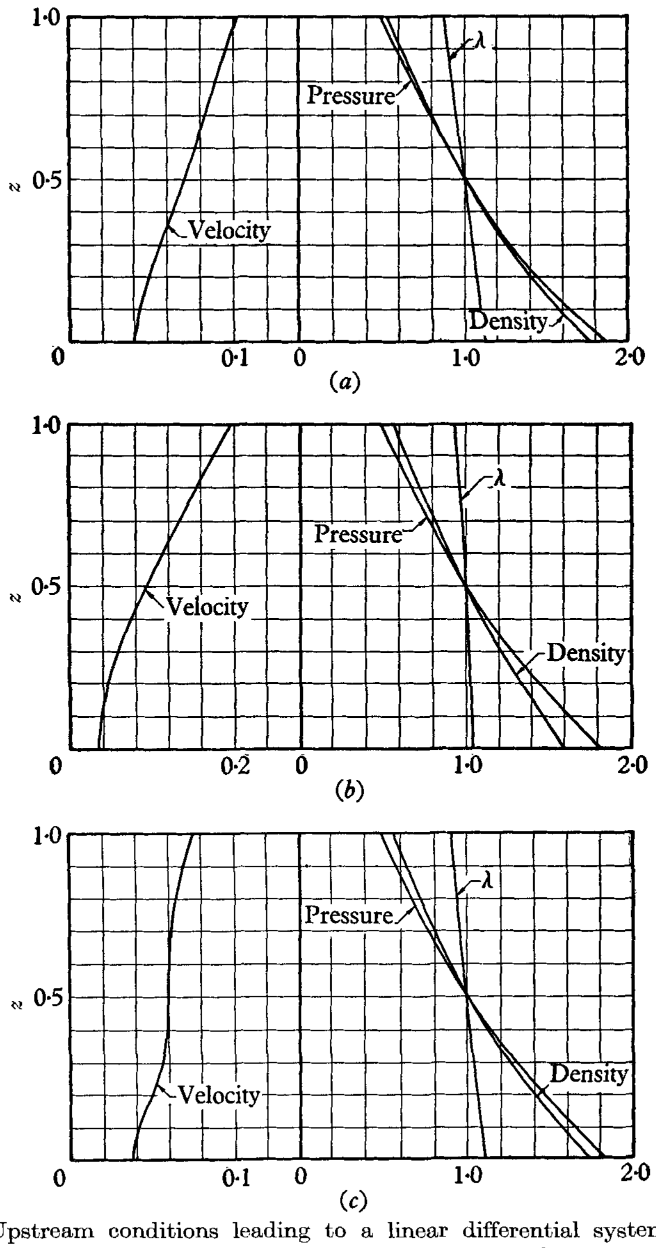

FIGURE 2. Upstream conditions leading to a linear differential system. (*a*) $A = 0$, $B = -3{\cdot}5$, $C-50{\cdot}0$, $D = 0$; (*b*) $A = -3{\cdot}00$, $B = -1{\cdot}00$, $C = -10{\cdot}00$, $D = -0{\cdot}02$; (*c*) $A = 10{\cdot}0$, $B = -3{\cdot}5$; $C = -50{\cdot}0$, $D = 0$.

4. Methods of solution

The basic problem can now be stated more accurately. Suitable values have been assigned to the constants A, B, C and D, and, out of the infinity of solutions of (15), an appropriate stream function $\psi_1'(z)$ has been selected corresponding to realistic upstream conditions. The problem is then to find a function $\psi'(x,z)$ satisfying equation (14), which is equal to zero on the lower boundary (consisting of the level portion $z = 0$ and the obstacle) and equal to $\psi_1'(1)$ on the upper boundary $z = 1$. Furthermore, $\psi'(x,z)$ should approach $\psi_1'(z)$ for $x \to -\infty$. Thus if we put

$$\psi'(x,z) = \psi_1'(z) + \mu\psi_2'(x,z), \tag{19}$$

in (14), the function $\psi_2'(x,z)$ has to satisfy the homogeneous equation (20), since $\psi_1'(z)$ is a solution of (15). Thus,

$$\nabla^2\psi_2' + \frac{1}{(\gamma-1)}\frac{\alpha}{(1-\alpha z)}\frac{\partial\psi_2'}{\partial z} + \beta(1-\alpha z)^{2/(\gamma-1)}(Az-C)\,\psi_2' = 0. \tag{20}$$

Furthermore, $\psi_2'(x,z)$ is subject to the conditions:

$$\psi_2'(x,z) = 0 \text{ on the lower boundary,} \tag{21}$$

$$\psi_2'(x,1) = 0, \tag{22}$$

$$\lim_{x\to-\infty} \psi_2'(x,z) = 0. \tag{23}$$

Prescription of the obstacle shape leads to a boundary condition for the stream function $\psi'(x,z)$ which is difficult to satisfy. This difficulty can be avoided as follows. We will use an indirect, but exact method for creating an obstacle and justify the procedure by the argument that the obstacle shape is of minor importance. Indeed, the main objective of the present study is the behaviour of the atmospheric flows in the lee of mountain ridges and the general characteristics of these flows should not be affected by the particular shape of the mountain profile. Two methods have been used to introduce a barrier. One is due to Yih and is a completely inverse method. A second method, due to Long, is semi-inverse in the sense that a barrier of infinitesimal height can be pre-assigned. Both methods involve the solution of equation (20), subject to the conditions $\psi_2'(x,0) = \psi_2'(x,1) = 0$. Of course, these two conditions do not uniquely determine a solution of (20), if singularities are allowed, as long as they are located inside the barrier. Indeed, the barrier is created by these singularities.

Equation (20) is satisfied by an expression of the form

$$e^{\pm\sqrt{\lambda_n}x} f_n(z), \tag{24}$$

where λ_n is an eigenvalue of the Sturm–Liouville system

$$\frac{d^2f}{dz^2} + \frac{1}{(\gamma-1)}\frac{\alpha}{(1-\alpha z)}\frac{df}{dz} + [\beta(1-\alpha z)^{2/(\gamma-1)}(Az-C)+\lambda]f = 0, \tag{25}$$

$$f(0) = f(1) = 0, \tag{26}$$

and $f_n(z)$ is the corresponding eigenfunction. The eigenvalues and corresponding orthonormal functions have been obtained by the use of power-series expansion and an iterative scheme. For certain combinations of values of A and C there may be negative eigenvalues. The exponential term in (24) becomes then a sine or cosine term. All eigenfunctions are normalized according to

$$\int_0^1 \frac{f_n^2(z)}{(1-\alpha z)^{1/(\gamma-1)}}\,dz = 1. \tag{27}$$

In the first method (Yih 1960*b*) the function $\psi_2'(x,z)$ is taken as an infinite series of terms of the type (24) with unknown coefficients A_n, B_n, C_n and D_n. However, the coefficients corresponding to $x < 0$ are different from the ones corresponding to $x > 0$. Furthermore, since $\psi_2'(x,z)$ has to approach zero for $x \to -\infty$, no oscillatory terms are allowed for $x < 0$, i.e. the summation for $x < 0$ begins with the first positive eigenvalue. Thus,

$$\psi_{2-}'(x,z) = \sum_{n=N+1}^{\infty} A_n e^{\sqrt{\lambda_n}x} f_n(z), \quad \text{for} \quad x < 0, \tag{28}$$

$$\psi_{2+}'(x,z) = \sum_{n=1}^{N} \{B_n \cos(-\lambda_n)^{\frac{1}{2}} x + C_n \sin(-\lambda_n)^{\frac{1}{2}} x\} f_n(z) + \sum_{n=N+1}^{\infty} D_n e^{-\sqrt{\lambda_n}x} f_n(z), \quad \text{for} \quad x > 0, \tag{29}$$

in which N is the number of negative eigenvalues of the Sturm–Liouville system consisting of (25) and (26).

Provided the series converge, both $\psi_{2-}'(x,z)$ and $\psi_{2+}'(x,z)$ satisfy equation (20) and the conditions (21) and (22). The function $\psi_{2-}'(x,z)$, valid for $x < 0$, vanishes for $x \to -\infty$ and thus satisfies (23). The coefficients A_n, B_n, C_n and D_n will now be determined to create a barrier on the lower boundary. It should be noted that the function $\psi_2'(x,z)$, consisting of $\psi_{2-}'(x,z)$ and $\psi_{2+}'(x,z)$, is analytic for $x < 0$ and $x > 0$ $(0 \leqslant z \leqslant 1)$, and the only singularities are located at $x = 0$. The fact, whether there will be singularities on the segment $x = 0$ $(0 \leqslant z \leqslant 1)$ depends, of course, on the choice of the coefficients A_n, B_n, C_n and D_n. If we were to select these coefficients in such a way as to make all points $(0, 0 \leqslant z \leqslant 1)$ regular, $\psi_2'(x,z)$ would be analytic throughout the whole strip $0 \leqslant z \leqslant 1$ and would necessarily have to be equal to zero, since periodic wave motion has been ruled by the assumption that waves do not occur far upstream. We will therefore allow the function $\psi_2'(x,z)$ to be singular on the portion $0 \leqslant z \leqslant a$ of the segment $0 \leqslant z \leqslant 1$. However, since no singularities can be tolerated in the flowfield, the created barrier should have a height of at least a at $x = 0$.

Different types of singularities can be used. For our calculations, a discontinuity in the x-derivative was introduced. Thus,

$$\psi_{2-}'(0,z) = \psi_{2+}'(0,z), \quad \text{for} \quad 0 < z < 1, \tag{30}$$

$$\frac{\partial\psi_{2-}'(0,z)}{\partial x} - \frac{\partial\psi_{2+}'(0,z)}{\partial x} = g(z), \quad \text{for} \quad 0 < z < a, \tag{31}$$

$$\frac{\partial\psi_{2-}'(0,z)}{\partial x} - \frac{\partial\psi_{2+}'(0,z)}{\partial x} = 0, \quad \text{for} \quad a < z < 1. \tag{32}$$

Equations (30) and (32) ensure the analyticity of $\psi_2'(x,z)$ on the segment $x = 0\,(a < z < 1)$ and therefore in the whole field of flow, and $\psi_{2+}'(x,z)$ is the analytic continuation of $\psi_{2-}'(x,z)$ outside the barrier. The conditions (30), (31) and (32) lead to

$$\sum_{n=N+1}^{\infty} A_n f_n(z) = \sum_{n=1}^{N} B_n f_n(z) + \sum_{n=N+1}^{\infty} D_n f_n(z), \tag{33}$$

$$\sum_{n=1}^{N} \sqrt{(-\lambda_n)}\, C_n f_n(z) - \sum_{n=N+1}^{\infty} \sqrt{\lambda_n}\,(A_n + D_n) f_n(z) = -g(z). \tag{34}$$

It follows from (33) that

$$B_n = 0 \quad (n = 1, 2, \ldots, N)$$

and

$$A_n = D_n \quad (n = N+1, N+2, \ldots),$$

and from (34) that

$$\sqrt{(-\lambda_n)}\, C_n = -\int_0^1 \frac{g(z) f_n(z)}{(1-\alpha z)^{1/(\gamma-1)}}\, dz \quad (n = 1, 2, \ldots, N)$$

and

$$\sqrt{\lambda_n}\,(A_n + D_n) = \int_0^1 \frac{g(z) f_n(z)}{(1-\alpha z)^{1/(\gamma-1)}}\, dz \quad (n = N+1, N+2, \ldots).$$

Indeed, the constants $\sqrt{(-\lambda_n)}\, C_n$ and $\sqrt{\lambda_n}\,(A_n + D_n)$ are merely the Fourier coefficients in the expansion of the function $g(z)$ in a series of eigenfunctions of the Sturm–Liouville system consisting of (25) and (26). The eigenfunctions corresponding to negative eigenvalues also appear in (34), so that all eigenfunctions must be present to make the expansion possible.

The final expressions for $\psi'_2(x, z)$ are thus

$$\psi'_{2^-}(x, z) = \frac{1}{2} \sum_{n=N+1}^{\infty} \frac{Q_n}{\sqrt{\lambda_n}}\, e^{\sqrt{\lambda_n} x} f_n(z), \quad \text{for} \quad x < 0 \tag{35}$$

and

$$\psi'_{2^+}(x, z) = -\sum_{n=1}^{N} \frac{Q_n}{\sqrt{(-\lambda_n)}} \sin(-\lambda_n)^{\frac{1}{2}} x f_n(z) + \frac{1}{2} \sum_{n=N+1}^{\infty} \frac{Q_n}{\sqrt{\lambda_n}}\, e^{-\sqrt{\lambda_n} x} f_n(z), \quad \text{for} \quad x > 0, \tag{36}$$

in which

$$Q_n = \int_0^a \frac{g(z) f_n(z)}{(1-\alpha z)^{1/(\gamma-1)}}\, dz.$$

The upper limit in the above integral has been taken equal to a since $g(z) = 0$ for $a < z < 1$. By changing the value of μ appearing in (19), the flow pattern can be changed. This value should be taken large enough so the barrier covers the segment $0 < z < a$ on $x = 0$. In this way the stream function will be analytic throughout the whole field of flow. The flow pattern is given by

$$\psi'(x, z) = \psi'_1(z) + \mu \psi'_{2^-}(x, z), \quad \text{for} \quad x < 0, \tag{37}$$

and

$$\psi'(x, z) = \psi'_1(z) + \mu \psi'_{2^+}(x, z), \quad \text{for} \quad x > 0. \tag{38}$$

In the method used by Long, the field of flow is divided into three regions ($x < -b$, $-b < x < b$, $x > b$), the middle-region ($-b < x < b$) containing the barrier. Although it is true that a flow pattern can be found for a barrier of arbitrary shape (however small), we will restrict ourselves to a barrier of the shape $\frac{1}{2}a\{1 + \cos(\pi x/b)\}$.

In each region, a homogeneous stream function is assumed each term of which satisfies equation (20). Thus,

$$\psi'_{2\mathrm{I}}(x, z) = \sum_{n=N+1}^{\infty} A_n e^{\sqrt{\lambda_n} x} f_n(z), \quad \text{for} \quad x < -b, \tag{39}$$

$$\psi'_{2\mathrm{II}}(x, z) = F_0(z) + F_1(z) \cos(\pi x/b) + \sum_{n=1}^{N} \{F_n \cos(-\lambda_n)^{\frac{1}{2}} x + G_n \sin(-\lambda_n)^{\frac{1}{2}} x\} f_n(z) + \sum_{n=N+1}^{\infty} (H_n e^{\sqrt{\lambda_n} x} + M_n e^{-\sqrt{\lambda_n} x}) f_n(z), \quad \text{for} \quad -b < x < b, \tag{40}$$

and $$\psi'_{2\text{III}}(x,z) = \sum_{n=1}^{N} \{B_n \cos(-\lambda_n)^{\frac{1}{2}} x + C_n \sin(-\lambda_n)^{\frac{1}{2}} x\} f_n(z)$$
$$+ \sum_{n=N+1}^{\infty} D_n e^{-\sqrt{\lambda_n} x} f_n(z), \quad \text{for} \quad x > b. \tag{41}$$

As far as regions I and III are concerned, each term in the series also satisfies the boundary conditions (21), in agreement with the fact that there is no obstacle in these regions. The terms $F_0(z)$ and $F_1(z) \cos(\pi x/b)$ appearing in (40) will cause the function $\psi'_{\text{II}}(x,z)$ to be different from zero on the line $z = 0$. Therefore the line $z = 0$ will not be a streamline in region II and an obstacle is thus created. Since the functions $F_0(z)$ and $F_1(z) \cos(\pi x/b)$ have to satisfy equation (20),

$$\frac{d^2F_0}{dz^2} + \frac{1}{(\gamma-1)} \frac{\alpha}{(1-\alpha z)} \frac{dF_0}{dz} + \beta(1-\alpha z)^{2/(\gamma-1)} (Az - C) F_0 = 0 \tag{42}$$

and $$\frac{d^2F_1}{dz^2} + \frac{1}{(\gamma-1)} \frac{\alpha}{(1-\alpha z)} \frac{dF_1}{dz} + [\beta(1-\alpha z)^{2/(\gamma-1)} (Az - C) - \pi^2/b^2] F_1 = 0. \tag{43}$$

Since the upper boundary ($z = 1$) has to remain a streamline, $F_0(z)$ and $F_1(z)$ must satisfy the conditions

$$F_0(1) = F_1(1) = 0. \tag{44}$$

Different values for $F_0(0)$ and $F_1(0)$ merely correspond to different obstacle shapes. It can be shown that when $F_0(0)$ and $F_1(0)$ are both taken equal to 1, the convergence of the series in the expressions (39), (40), and (41) is most rapid. We therefore put

$$F_0(0) = F_1(0) = 1. \tag{45}$$

The integration of equations (42) and (43) subject to the conditions (44) and (45) has been performed using power-series expansions. It was tacitly assumed that neither 0 nor π^2/b^2 is equal to an eigenvalue of the Sturm–Liouville system consisting of (25) and (26). It would then indeed be impossible to find solutions of equations (42) and (43) satisfying conditions (44) and (45). The coefficients $A_n, B_n, C_n, D_n, F_n, G_n, H_n$ and M_n are now used to establish continuity of $\psi'(x,z)$ and $\partial\psi'(x,z)/\partial x$ at the lines $x = -b$ and $x = +b$, making the function $\psi'(x,z)$ analytic throughout the whole field of flow. In order to accomplish this, the functions $F_0(z)$ and $F_1(z)$ have to be expanded in a series of eigenfunctions $f_n(z)$ Thus,

$$F_0(z) = \sum_{n=1}^{\infty} C_n^0 f_n(z), \tag{46}$$

and $$F_1(z) = \sum_{n=1}^{\infty} C_n^1 f_n(z). \tag{47}$$

The coefficients C_n^0 and C_n^1 are given by

$$C_n^0 = \int_0^1 \frac{F_0(z) f_n(z)}{(1-\alpha z)^{1/(\gamma-1)}} dz, \tag{48}$$

and $$C_n^1 = \int_0^1 \frac{F_1(z) f_n(z)}{(1-\alpha z)^{1/(\gamma-1)}} dz. \tag{49}$$

The integrals appearing in (48) and (49) can be evaluated easily by observing that the functions $F_0(z)$ and $F_1(z)$ satisfy (42) and (43) and the boundary conditions (44) and (45). The coefficients C_n^0 and C_n^1 are found to be

$$C_n^0 = \frac{1}{\lambda_n}\frac{df_n(0)}{dz},$$

and

$$C_n^1 = \frac{1}{\lambda_n + (\pi^2/b^2)}\frac{df_n(0)}{dz}.$$

The requirement that $\psi'(x,z)$ and $\partial\psi'(x,z)/\partial x$ be continuous at $x = -b$ and $x = b$ determines the values of the coefficients. These values are

$$\begin{aligned}
A_n &= D_n = -R_n \sinh\sqrt{\lambda_n}\, b, && \text{for } n > N,\\
H_n &= M_n = \frac{R_n}{2} e^{-\sqrt{\lambda_n} b}, && \text{for } n > N,\\
B_n &= 0, && \text{for } n \leqslant N,\\
C_n &= -2R_n \sin(-\lambda_n)^{\frac{1}{2}} b, && \text{for } n \leqslant N,\\
F_n &= R_n \cos(-\lambda_n)^{\frac{1}{2}} b, && \text{for } n \leqslant N,\\
G_n &= -R_n \sin(-\lambda_n)^{\frac{1}{2}} b, && \text{for } n \leqslant N,
\end{aligned}$$

in which $R_n = C_n^1 - C_n^0$, or

$$R_n = -\frac{\pi^2}{b^2}\frac{df_n(0)}{dz}[\lambda_n\{\lambda_n + (\pi^2/b^2)\}]^{-1}. \tag{50}$$

Equations (39), (40) and (41) become

$$\psi'_{2\text{I}}(x,z) = -\sum_{n=N+1}^{\infty} R_n \sinh\sqrt{\lambda_n}\, b\, e^{\sqrt{\lambda_n} x} f_n(z), \tag{51}$$

$$\begin{aligned}
\psi'_{2\text{II}}(x,z) = F_0(z) + F_1(z)\cos(\pi x/b) &+ \sum_{n=1}^{N} R_n \cos\{(-\lambda_n)^{\frac{1}{2}}(b+x)\} f_n(z)\\
&+ \sum_{n=N+1}^{\infty} R_n e^{-\sqrt{\lambda_n} b}\cosh(\sqrt{\lambda_n} x) f_n(z),
\end{aligned} \tag{52}$$

$$\begin{aligned}
\psi'_{2\text{III}}(x,z) = -2\sum_{n=1}^{N} R_n \sin\sqrt{(-\lambda_n)}\, b \sin\{(-\lambda_n)^{\frac{1}{2}} x\} f_n(z)\\
- \sum_{n=N+1}^{\infty} R_n \sinh\sqrt{\lambda_n}\, b e^{-\sqrt{\lambda_n} x} f_n(z).
\end{aligned} \tag{53}$$

The stream function $\psi'(x,z)$ from which the flow pattern can be obtained is then $\psi'(x,z) = \psi'_1(z) + \mu\psi'_2(x,z)$, in which $\psi'_2(x,z)$ is taken equal to $\psi'_{2\text{I}}(x,z)$, $\psi'_{2\text{II}}(x,z)$, $\psi'_{2\text{III}}(x,z)$ respectively, in the regions $x < -b$, $-b < x < b$, $x > b$.

5. Discussion of results

The reference point, at which the pressure and density are equal to p_0 and ρ_0, respectively, has been chosen in the middle of the troposphere, that is at $z = 0{\cdot}5$. The following values have been taken: $p_0 = 410$ mm Hg, and $\rho_0 = 0{\cdot}000723$ g/cm^3. The height of the tropopause has been taken to be 10 km. The average value of the specific energy H' used in the calculations was obtained by evaluating this quantity at the reference point $z = 0{\cdot}5$,

$$H' = 3{\cdot}198 + \tfrac{1}{2}U^2 \approx 3{\cdot}2.$$

With $\gamma = 1{\cdot}4$, the coefficients α and β then become $\alpha = 0{\cdot}3125$, $\beta = 2{\cdot}3471$. With these numerical values, several upstream conditions have been obtained. The density, pressure and temperature profiles approximate the realistic profiles in the atmosphere closely. This is hardly surprising if one considers the

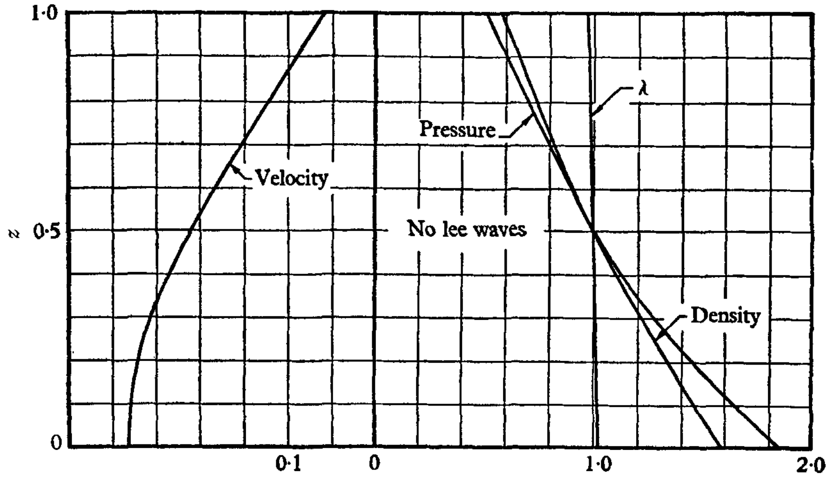

FIGURE 3. Upstream conditions leading to a flow pattern with no lee-wave components.

fact that the stratifications in entropy and specific energy occurring in the atmosphere are rather slight and we have chosen the constants A, B, C and D in such a way as to satisfy these latter conditions. Although the velocity term $(\frac{1}{2}U'^2)$ was included in equation (17) to determine the pressure variation (with height), quite large velocity changes have a rather limited influence on the pressure profile. Various upstream conditions (including the wind profiles) corresponding to various wave formations in the lee are shown in figures 3, 5 and 9. All the examples shown correspond to an entropy increasing with height (or λ decreasing with height), as is required by static stability. The essential task is to find some combinations of stratifications in entropy and specific energy together with compatible velocity profiles that give rise to either no lee waves or lee waves with one or more components. By reducing the velocity far upstream and leaving the other quantities unaltered, it is possible to create more lee-wave components. Indeed, once A and C are chosen the number of lee-wave components (corresponding to the negative eigenvalues) is fixed. Decreasing the velocity, which is equivalent to reducing the stream function, then results in a smaller stratification. The extreme case (zero velocity upstream and no stratification) can be considered as the limit case of a flow with several wave components in the lee.

Figure 4 shows a flow pattern with no waves in the lee. The obstacle is symmetric, as expected. The solution has been obtained by Yih's method. Mathematically, a solution is allowed for any height of the obstacle in agreement with the fact that there are no lee waves present. Indeed, once a particular height h of the obstacle has been selected the coefficient μ appearing in (19) is given by

$$\mu = -\frac{\psi_1'(h)}{\psi_2'(0,h)}. \tag{54}$$

If $\psi_2'(x,z)$ does not have any nodal lines and therefore $\psi_2'(0,z) \neq 0$ for $0 < z < 1$, equation (54) yields a value of μ for any height h between 0 and 1. In the case of

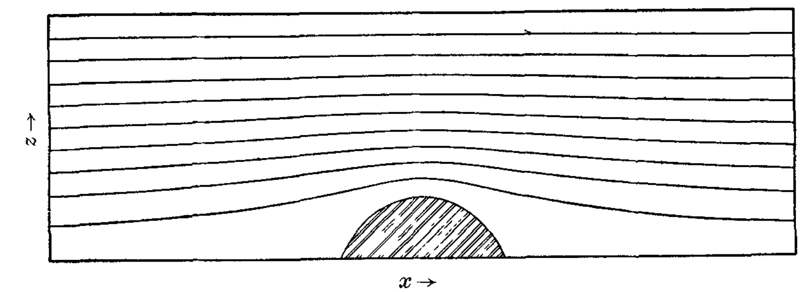

FIGURE 4. Flow pattern with no lee waves.

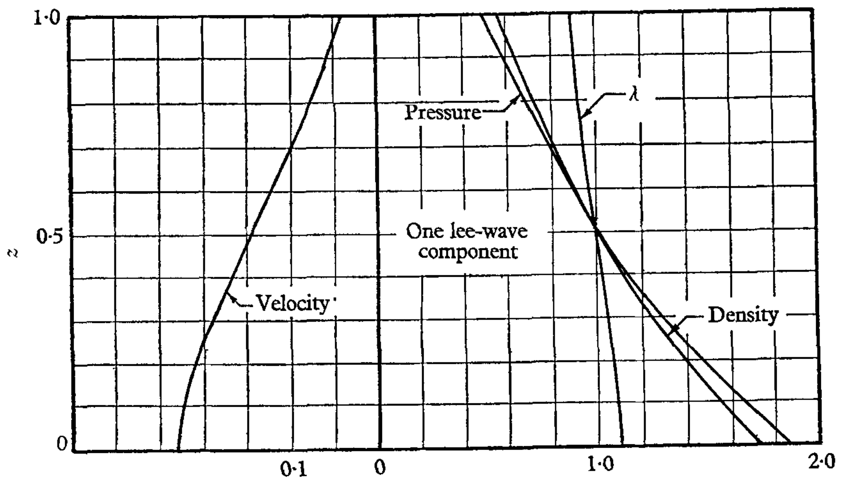

FIGURE 5. Upstream conditions leading to a flow pattern with one lee-wave component. $A = 0$, $B = -2{\cdot}5$, $C = -30{\cdot}0$, $D = 0$.

one lee-wave component (say), the function $\psi_2'(x,z)$ has one nodal line and there exists a number z_1 between 0 and 1 such that $\psi_2'(0,z_1) = 0$. Equation (54) still yields a value of μ provided $h < z_1$. The obstacle height approaches z_1, as μ approaches infinity. It is thus impossible to obtain a steady flow past an obstacle of a height greater than the height of the nodal line.

Figure 6 represents a flow pattern where the coefficients A and C have been selected to give rise to one wave component in the lee. The usual jet occurring above the barrier and extending upstream is present. The much stronger wave motion in the lower part of the channel should not be considered merely (if at all) as a result of compressibility. One of the reasons certainly is the shape of the velocity profile far upstream. It may be conjectured that a higher velocity in the upper part of the channel has a 'washing down' effect on the waves. Indeed, as pointed out earlier, increasing the velocity at constant stratification tends to eliminate wave motion. The influence of the velocity profile on the development of the waves as a function of height may become clearer by the following consideration. If the velocity increases with height, the graph representing the stream function $\psi_1'(z)$ upstream is curved downward (see figure 7). This means that a moderate value (represented by the segment AB in figure 7) of the

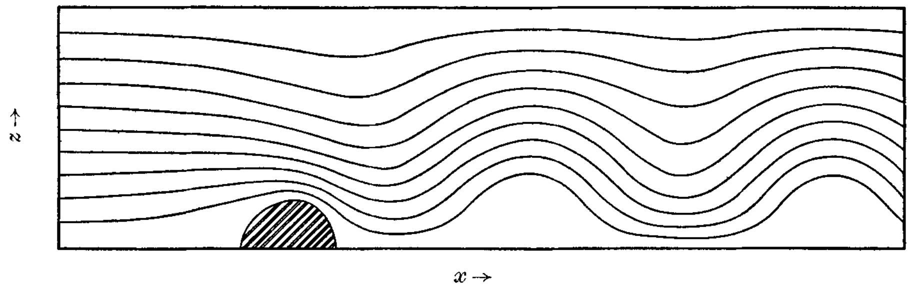

FIGURE 6. Flow pattern with one lee-wave component.

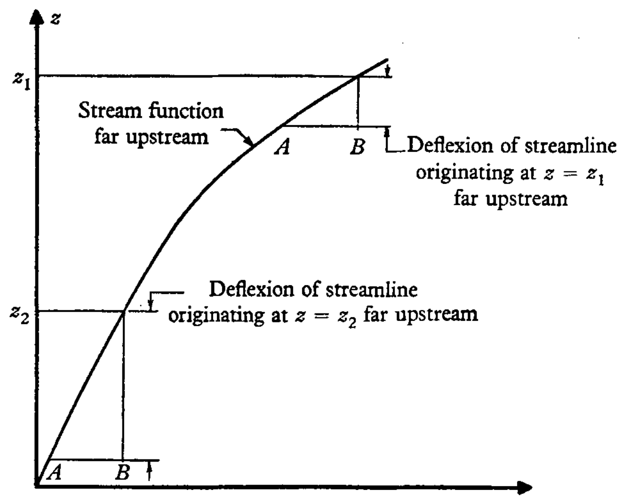

FIGURE 7. Influence of wind profile on wave amplitude.

stream function $\psi_2'(x, z)$ will cause a rather large deflexion of the relevant streamline when one considers the lower part of the channel, while the same value of $\psi_2'(x, z)$ would only cause small deviations in the upper part of the channel. This would indicate that such a velocity profile (velocity increasing with height) favours the wave development near the ground. The opposite conclusions are reached if velocity profiles are considered where the velocity decreases with height.

The isothermal lines corresponding to the flow of figure 6 are shown in figure 8. The temperature can easily be calculated from

$$T = \frac{H' - \lambda z}{\lambda E}, \tag{55}$$

in which the velocity term has been neglected. It can be seen from the figures 6 and 8 that an air particle in its up and down motion will have a varying temperature. These temperature changes are, of course, due to isentropic compression and expansion. A short numerical calculation reveals that the temperature of a particle following the lower streamline (originating at $z = 0{\cdot}1$ far upstream) changes from 15 to $-11\,^{\circ}\mathrm{C}$. This partially explains the formation of equally

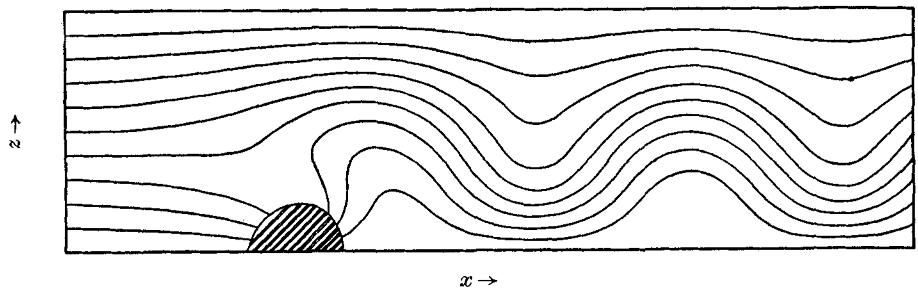

FIGURE 8. Isothermal lines in the flow with one lee-wave component.

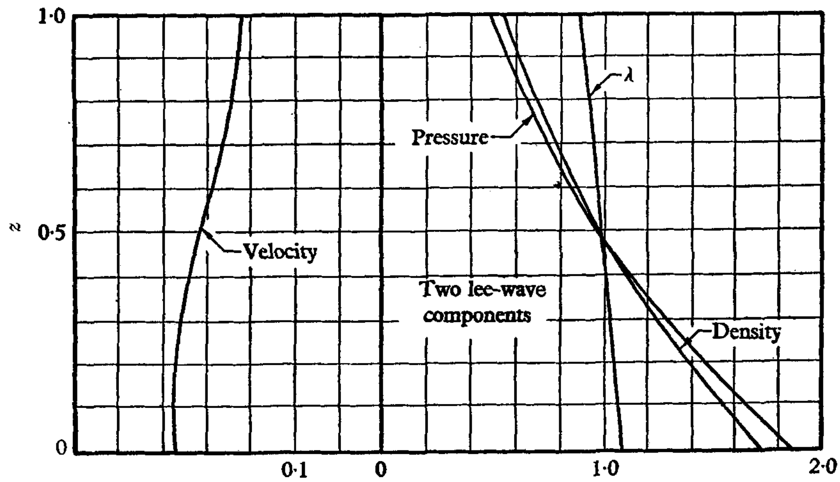

FIGURE 9. Upstream conditions leading to a flow pattern with two lee-wave components.

spaced clouds as has sometimes been observed in the lee of mountain ridges. If the humidity of the air is such that the saturation point is reached in the vicinity of the crests of the waves, apparently stationary clouds would be formed. However, in the case of humid air, the results are only qualitatively true since the basic assumption, λ constant along a streamline, becomes questionable when the medium undergoes a partial change of state.

Figure 10 shows a pattern with two lee-wave components and was obtained using Long's method. The formation of two jets, one downward and one upward, is apparent. The downward jet is more developed for reasons pointed out earlier. Although no closed cells appear, they could be created by increasing the height of the obstacle. However, the flow inside these cells, as obtained by the previous analysis, is not *a priori* justifiable because the streamlines in the eddies do not originate far upstream and consequently the upstream conditions do not determine the values of λ and H' on these streamlines. Care has been taken to keep the obstacle height below a certain limit in order to avoid extremely converging streamlines since these would lead to high velocities and the validity of neglecting the dynamic compressibility might become questionable.

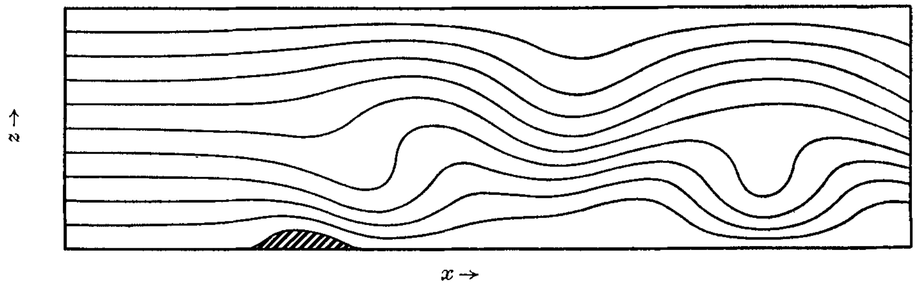

FIGURE 10. Flow pattern with two lee-wave components.

6. Comparison with flow of an incompressible fluid

In order to bring out the effect of compressibility an attempt has been made to obtain a flow of a compressible fluid and a flow of an incompressible fluid, both with equivalent upstream conditions (what is meant here by 'equivalent' will be explained later). We know that for the governing differential system to be linear, an inverse procedure has to be adopted as indicated in §3. This makes a complete match of upstream conditions of two different flows (compressible and incompressible) impossible. Since the theory dealing with the flow of an incompressible stratified fluid will be needed, a brief summary of the equations in dimensionless form is given below. For more details we refer to Yih (1960*b*). The associated velocity field (u', w') is related to the original velocity field (u, w) by means of $u' = u\sqrt{\rho}$ and $w' = w\sqrt{\rho}$. These two velocity components (u', w') can be derived from the stream function $\psi'(x, z)$ by $u = \partial\psi'/\partial z$ and $w' = -\partial\psi'/\partial x$. The stream function satisfies the equation

$$\nabla^2\psi' + z\frac{d\rho}{d\psi'} = \frac{dH'}{d\psi'}, \tag{56}$$

in which

$$H' = p + \tfrac{1}{2}\rho(u^2 + w^2) + \rho z. \tag{57}$$

Equation (56) can again be made linear by assuming linear functions of ψ' for $d\rho/d\psi'$ and $dH'/d\psi'$. The most general, but linear, case leads to Bessel functions of fractional order. In some cases, however, the solution can be expressed in terms of trigonometric and exponential functions. This is the case when far upstream, we choose the density as a linear function of height, and the associated velocity constant. Thus, far upstream the conditions are prescribed by

$$\rho = 1 + a(1 - 2z); \quad U' = U'_0, \tag{58}$$

where a and U'_0 are constants as indicated on figure 11. Then $\psi'_1 = U'_0 z$ and

$$\frac{d\rho}{d\psi'} = \frac{d\rho}{dz}\frac{1}{U'_0} = -\frac{2a}{U'_0}. \tag{59}$$

The term $dH'/d\psi'$ becomes

$$\frac{dH'}{d\psi'} = \frac{1}{U_0'}\frac{dH'}{dz} = \left(\frac{dp}{dz}+\rho+z\frac{d\rho}{dz}\right)\frac{1}{U_0'} = z\frac{d\rho}{dz}\frac{1}{U_0'}.$$

So, with $d\rho/dz = -2a$ by virtue of (58),

$$\frac{dH'}{d\psi'} = -\frac{2a}{U_0'}z = -\frac{2a}{U_0'^2}\psi'. \tag{60}$$

Far upstream, equation (56) becomes

$$\frac{d^2\psi_1'}{dz^2}+\frac{2a}{U_0'^2}\psi_1' = \frac{2az}{U_0'}. \tag{61}$$

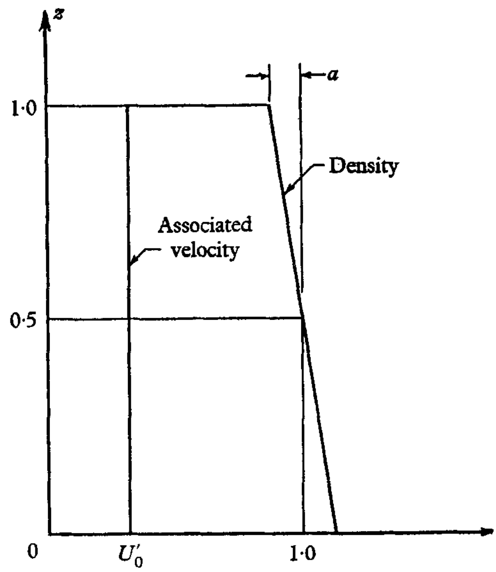

FIGURE 11. Upstream conditions for an incompressible fluid and leading to equation (61).

The general solution is

$$\psi_1'(z) = C_1 \sin\left(\frac{(2a)^{\frac{1}{2}}}{U_0'}z+C_2\right)+U_0'z. \tag{62}$$

The velocity U' is given by

$$U'(z) = \frac{(2a)^{\frac{1}{2}}}{U_0'}\left[C_1\cos\left(\frac{(2a)^{\frac{1}{2}}}{U_0'}z+C_2\right)\right]+U_0'. \tag{63}$$

We see that, although equation (61) was obtained from a linear density stratification and constant associated velocity far upstream, a whole class of velocity profiles, given by (63), and corresponding density stratifications lead to the same differential equation for the stream function. Furthermore, any arbitrary constant may be added to the stream function and will not change the velocity profile. The stream function is then governed by an equation which differs from equation (61) by a constant in the right-hand member. This flexibility will be used to get a closer match between the incompressible and compressible flow.

By adjusting the values of the coefficients A, B, C and D in the case where compressibility is taken into account, a velocity profile (see figure 12) has been obtained which can be matched closely by a function of the form given by (63). The density variation is of course considerable and corresponds roughly to normal atmospheric conditions. If we use an incompressible fluid in an attempt to describe the flow of a compressible one, there is some question as to what density stratification should be taken far upstream. It is indeed the combined action of density difference and gravity that determines the restoring forces necessary for the creation of waves. The fact that the same density stratification in both compressible and incompressible fluid will give rise to different restoring forces can

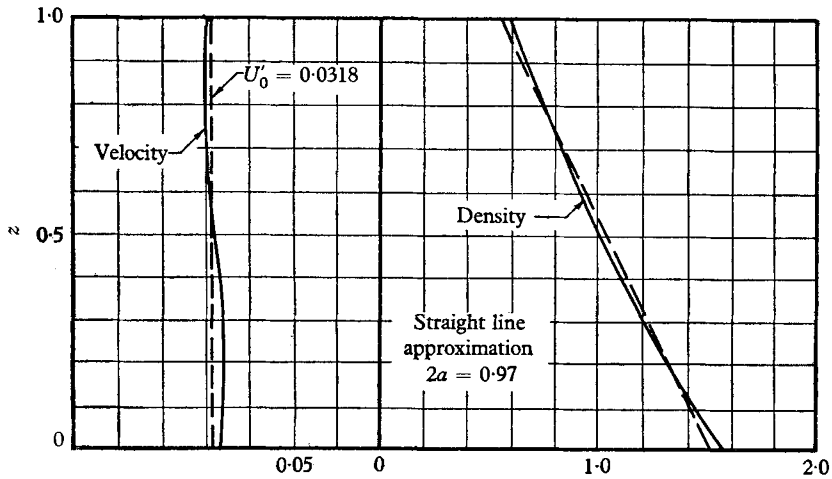

FIGURE 12. Upstream conditions used for the comparison between the flow of an incompressible fluid and that of a compressible fluid. $A = 11$, $B = -1$, $C = -19$, $D = 0$.

easily be inferred from the following reasoning. The density of a particle of air increases as the particle goes down (due to compression) and decreases when it goes up (due to expansion), whereas the density of a particle of an incompressible fluid is independent of its location.

Besides, the following numerical calculation already predicts the marked difference in behaviour between the flow of a compressible and an incompressible fluid, the density stratification being taken equal in both cases.

If we roughly approximate the density stratification, as shown in figure 12, by a straight line and the velocity profile by a constant, we find for the values of a and U_0' appearing in equation (61), $a = 0{\cdot}485$ and $U_0' = 0{\cdot}0318$. Equation (61) then becomes

$$\frac{d^2\psi_1'}{dz^2} + 959\psi_1' = 30{\cdot}5z.$$

This indicates that the resulting flow pattern would contain 9 lee-wave components while the corresponding flow of the fluid being considered compressible contains only a single wave component.

An appropriate density stratification (for an incompressible fluid) is such that the action of gravity leads to the same restoring forces in both the compressible and incompressible flow. The so-called potential density

$$\rho_{*_p} = \rho_0 \exp\{(S_0 - S_*)/c_p\}$$

satisfies this requirement.

The potential density can be written in the dimensionless form

$$\frac{\rho_{*_p}}{\rho_0} = \exp\{(S_0 - S_*)/c_p\} = \frac{\rho_*}{\rho_0}\left(\frac{p_0}{p_*}\right)^{1/\gamma} = \lambda,$$

which demonstrates the significance of the variable λ.

In the case of the incompressible fluid, an ideal choice of the upstream conditions consists of a velocity profile identical to the velocity in the compressible flow (figure 12), and a density stratification the same as the potential density stratification (figure 13) prevailing in the compressible fluid.

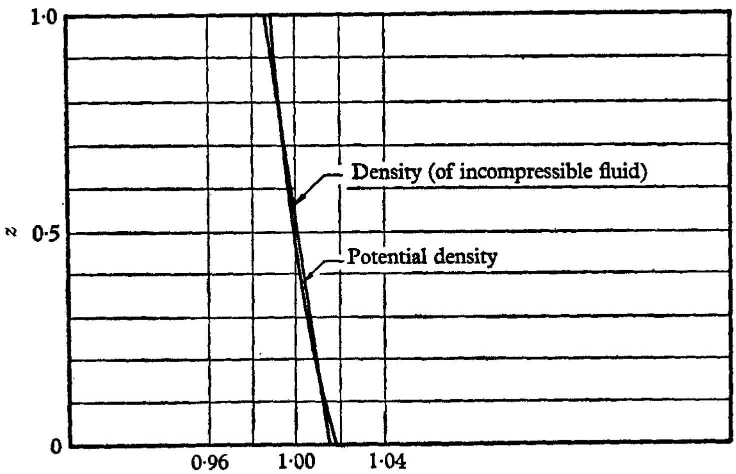

FIGURE 13. Approximation to the stratification of potential density in a compressible fluid by the density stratification in an incompressible fluid. Both stratifications lead to linear governing equations.

These quantities can be approximated rather closely by taking $a = 0{\cdot}01345$, $U_0' = 0{\cdot}0318$, $C_1 = 0{\cdot}000318$ and $C_2 = -1{\cdot}0315$ in equation (63). The velocity profile is then given by

$$U'(z) = 0{\cdot}00164 \cos(5{\cdot}1576z - 1{\cdot}0315) + 0{\cdot}0318.$$

This profile is so close to the one shown in figure 12 that the two graphs practically coincide. The stream function has been evaluated from equation (62) and is given by

$$\psi_1'(z) = 0{\cdot}000318 \sin(5{\cdot}1576z - 1{\cdot}0315) + 0{\cdot}0318z.$$

The density stratification then is

$$\rho(z) = -(2a/U_0')\,\psi_1'(z) + \text{const.} = -0{\cdot}8459\psi'(z) + 1{\cdot}0157.$$

This stratification is almost linear and is shown, as a basis for comparison, in figure 13. Inserting the numerical values of a and U_0' in the expressions (59) and (60), we obtain

$$d\rho/d\psi' = -0{\cdot}8459 \quad \text{and} \quad dH'/d\psi' = -26{\cdot}601\psi'.$$

Equation (56) becomes

$$\nabla^2\psi' + 26{\cdot}601\,\psi' = 0{\cdot}8459z. \tag{64}$$

The resulting flow pattern has been obtained by Long's method since this method allows us to control both the width and the height of the obstacle (figure 14). The corresponding flow pattern of the compressible fluid is shown in figure 15.

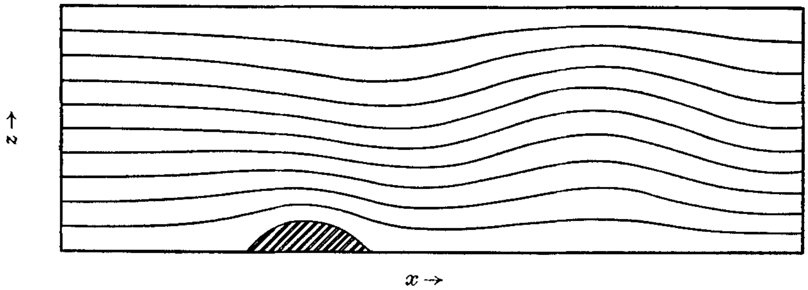

FIGURE 14. Comparison between the flow of an incompressible and a compressible fluid. Incompressible case.

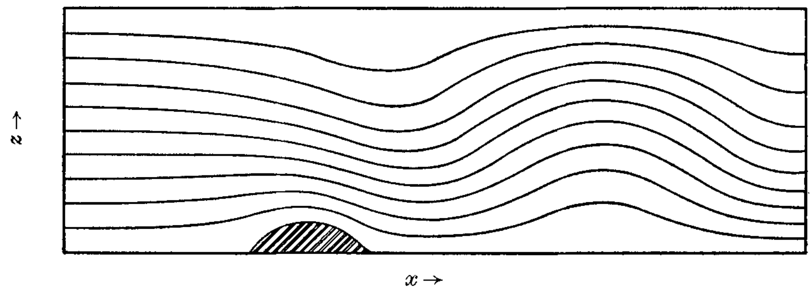

FIGURE 15. Comparison between the flow of an incompressible and a compressible fluid. Compressible case.

The Sturm–Liouville system resulting from the separation of variables in equation (64) admits one negative eigenvalue and, hence, one lee-wave component is present in the flow pattern. It is interesting that the negative eigenvalue in the case of the compressible fluid is nearly equal to the negative eigenvalue corresponding to the incompressible flow. Indeed the latter is

$$\lambda_1 = \pi^2 - 26{\cdot}601 = -16{\cdot}731,$$

while the corresponding numerical value in the case of the compressible fluid was found to be $-16{\cdot}078$. This means that the wavelengths in both flow patterns are nearly equal as can be seen from figures 14 and 15. However, in spite of the fact that the obstacles in both cases (compressible and incompressible) are nearly equal, the wave motion is of larger amplitude in the case of the compressible fluid. Indeed, the maximum vertical oscillation of a streamline in the compressible flow is approximately 0·29, whereas the corresponding oscillation in the incompressible flow is roughly 0·165. The jet extending upstream is markedly more convergent in the compressible flow than in the incompressible one.

It is interesting to observe the behaviour of the lower streamline (originating at $z = 0{\cdot}1$ far upstream) in both cases. Both streamlines have approximately the same shape upstream of the trailing edge of the obstacle. Downstream from the obstacle, however, the maximum vertical oscillation of this streamline is, in the case of the compressible fluid, more than three times as large as the corresponding oscillation in the case of the incompressible fluid. Thus, if an incompressible fluid is used for the study of atmospheric flows, the flow pattern obtained becomes questionable in the lower atmosphere. In particular it may happen that the incompressible flow would not display any eddies while these eddies may be present in the flow of the compressible fluid.

7. Conclusions

Large-amplitude motion in steady, two-dimensional atmospheric flows past mountain ridges has been studied. For certain upstream conditions, the governing equation was exactly linear in the case of slight stratification in entropy and specific energy. These upstream conditions leave wind profile and density stratification (or the stratification of any other relevant physical quantity) quite flexible and it is possible to approximate existing atmospheric conditions rather closely.

A general criterion governing the presence of lee waves and expressed in terms of wind velocity and entropy stratification would be highly complicated. In a flow where, say, one lee-wave component is present, it is possible for the wavelength to remain the same and this with varying stratification in entropy. This variation in stratification does not uniquely determine a change in wind profile, even if the wavelength of the wave component is to be kept constant. However, roughly we can state that an increase in entropy stratification favours wave development whereas increasing the wind velocity tends to eliminate wave motion.

All the obtained flow patterns where waves in the lee are present show one or more jets extending upstream. Furthermore, they (the flow patterns) exhibit a tendency to develop downstream eddies. The presence of these eddies depends on the height of the ridge. Increasing this height may also lead to the formation of closed cells but the flow inside these cells, as calculated here, cannot be justified since the relevant streamlines do not originate far upstream.

The temperature field corresponding to a particular flow pattern (one lee-wave component) shows the existence of cold regions near the crests of the waves which partly explains the formation of equally spaced clouds sometimes observed in the lee of mountain ridges.

The comparison between an atmospheric flow, the air being considered compressible, and a flow of an incompressible fluid reveals clearly that, in order to approximate the flow of a compressible fluid by that of an incompressible one, the density stratification for the incompressible fluid should be taken equal to the stratification of potential density in the atmosphere. Under similar upstream conditions the flows of the compressible and incompressible fluids have then the same general characteristics. In particular, the waves present in both flows have nearly the same wavelength. However, the spacing of the streamlines is more varied in the compressible flow and the wave is more developed. In particular, the amplitude of the wave in the lower atmosphere is approximately three times as large as the corresponding amplitude in the incompressible flow.

The author wishes to express his appreciation to Professor Chia-Shun Yih who suggested the problem and under whose direction at the University of Michigan the work was performed. The research was partially sponsored by the Army Research Office (Durham) through a contract with the University of Michigan. The support of the Institute of Science and Technology in the form of a predoctoral fellowship is much appreciated.

REFERENCES

CRAPPER, G. D. 1959 A three dimensional solution for waves in the lee of mountains. *J. Fluid Mech.* **6**, 51–76.

LONG, R. R. 1953*a* Some aspects of the flow of stratified fluids. I. A theoretical investigation. *Tellus*, **5**, 42–7.

LONG, R. R. 1953*b* Some aspects of the flow of stratified fluids. III. Continuous density gradients. *Tellus*, **7**, 342–57.

LONG, R. R. 1953*c* Models of small-scale atmospheric phenomena involving density stratification. *Fluid Models in Geophysics*, pp. 135–47. Washington: U.S. Gov. Printing Office.

LYRA, G. 1943 Theorie der stationären Leewellenströmung in freier Atmosphäre. *Z. angew. Math. Mech.* **23**, 1–28.

QUENEY, P. 1947 Theory of perturbations in stratified currents with applications to air flow over mountain barriers. *Misc. Rep. No.* 23, *Dept. Met., Univ. Chicago.*

QUENEY, P. 1948 The problem of air flow over mountains: a summary of theoretical results. *Bull. Amer. Met. Soc.* **29**, 16–25.

SCORER, R. S. 1949 Theory of waves in the lee of mountains. *Quart. J.R. Met. Soc.* **75**, 41–56.

SCORER, R. S. 1953 Theory of air flow over mountains: II. Flow over a ridge. *Quart. J.R. Met. Soc.* **79**, 70–83.

SCORER, R. S. 1954 Theory of air flow over mountains: III. Airstream characteristics. *Quart. J.R. Met. Soc.* **80**, 417–28.

SCORER, R. S. & WILKINSON, M. 1956 Waves in the lee of an isolated hill. *Quart. J.R. Met. Soc.* **82**, 419–27.

YIH, C. S. 1960*a* A transformation for non-homentropic flows with an application to large amplitude motion in the atmosphere. *J. Fluid Mech.* **9**, 68–90.

YIH, C. S. 1960*b* Extract solutions for steady two-dimensional flow of a stratified fluid. *J. Fluid Mech.* **9**, 161–74.